

# SPATIAL ERROR CONCEALMENT TECHNIQUE USING VERGE POINTS

Yizhi Gao<sup>†</sup>, Jin Wang<sup>††</sup>, Yunqiang Liu<sup>††</sup>, Xiaokang Yang<sup>†</sup> and Jia Wang<sup>†</sup>

<sup>†</sup> Institute of Image Communication and Information Processing,  
Shanghai Jiao Tong University, Shanghai, P.R.China

<sup>††</sup> Philips Research East Asia, Shanghai, P.R.China

## ABSTRACT

This paper presents a spatial error concealment technique using “verge points” which are the high-curvature points on image surfaces. Associated with curvature information, the verge points provide important characteristics in reconstructing broken edges. In our method, only a single layer of verge points surrounding the missing area are extracted. The broken edges are reconstructed by pairing these verge points with respect to both the curvature information and their neighboring pixel values. Simulations show that with our pairing criterion, most of the object edges are recovered and our concealment technique yields satisfactory results especially in terms of subjective perception.

**Index Terms**— Error concealment, spatial interpolation

## 1. INTRODUCTION

Spatial error concealment (SEC) is often adopted for intra coded frame or areas of low temporal redundancy in inter-coded frames [1]. The existing spatial EC algorithms include bilinear interpolation [2], multi-directional interpolation [3], maximally smooth recovery [4], non-uniform rational B-spline interpolation [5], geometric-structure-based EC [6], orientation adaptive sequential interpolation [7], and classification-based SEC method [8].

In this paper, we propose a spatial EC technique by recovering the edges in the first place. Instead of performing edge detection in enlarged regions as in [9][10], only a single layer of “verge points” surrounding the corrupted area are extracted. The concept of “verge point” (VP) was raised originally in [11] for representing images using points on image surfaces. These so-called verge points are those controlling the curvature of intensity profile with which the image surface can be represented. In existing literature, the pairing of broken edges remains a challenging problem while extending them requires even more precise information. The proposed method selects the best pairing from a limited number of candidates considering the consistency of both curvature information and neighboring pixel values. We take advantage of the information

associated with VP (sign, curvature intensity and tangential angle) so as to reconstruct the missing VP in damaged areas and then recover the non-verge points by interpolation from the nearest VPs or correctly received pixels. Our simulations show that by reasonably reconstructing the verge points, most of the object edges are preserved in a simple but subjectively effective way.

## 2. CONCEPT OF VERGE POINTS

This section reviews the concept of verge point introduced in [11]. In representing an image surface (with the intensity considered as the third dimension), verge points are located at high-curvature areas in terms of local intensity changing. Every verge point is associated with a curvature intensity which presents the locally maximal rate of intensity change [12], denoted as  $k$ . The corresponding direction  $\Lambda_1$  is called the direction of maximal intensity change as shown in Fig. 1. What is more interesting in our problem,  $\Lambda_2$  presents the important information of tangential angle, which will be denoted as  $\theta_2$  in the following sections. In addition, verge points are signed. Positive signs mean that the intensity increases along the direction of  $\Lambda_1$  while negative signs correspond to decreases. Therefore, along the edges as in Fig. 1, two arrays of verge points, respectively with positive and negative sign, are extracted.

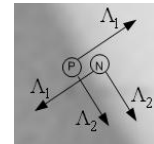


Fig. 1 Verge points signed with positive (P) and negative signs (N);  $\Lambda_1$  and  $\Lambda_2$  present directions of maximal and minimal intensity change respectively.

## 3. PROPOSED ALGORITHM

As described in the previous part, every verge point is characterized by its pixel value  $f(x,y)$ , curvature sign  $S(x,y)$ , curvature intensity  $k(x,y)$  and its tangential angle  $\theta_2(x,y)$ . Based on the assumption that for low-curvature edges (e.g. straight lines in images), these parameters remain quasi-constant along the edge direction, we exploit this spatial

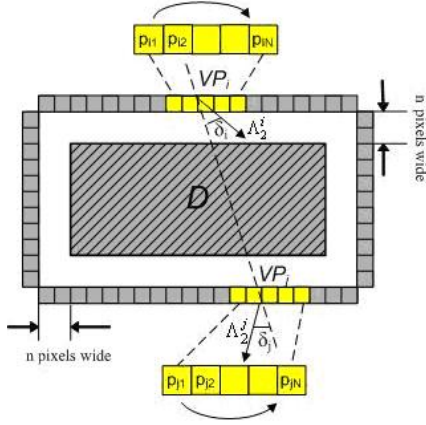


Fig. 2 Verge points of  $n$ -pixel distance from the border of the damaged area  $D$  (in slashes). Pixels  $p_{i1}p_{i2}\dots p_{iN}$  and  $p_{j1}p_{j2}\dots p_{jN}$  are the neighboring pixels centered at  $VP_i$  and  $VP_j$  respectively (numbered clockwise and counterclockwise respectively).  $\delta_i$  is the angle between the tangential vector  $\Lambda_2^i$  and the segment connecting  $p_i$  and  $VP_i$ .

redundancy hereafter to reconstruct the edges in the missing areas.

### 3.1. Verge point pairing

For a corrupted area  $D$  (Fig. 2), its surrounding verge points are first extracted. Practically, as several layers of its immediate neighbors are excluded from the verge point calculation (due to Gaussian convolution and the differentiation operations [11]), the verge points of  $n$ -pixel distance from the borders are extracted instead, where  $n$  depends on the Gaussian filter window size. We apply a  $3 \times 3$  Gaussian filter and thus set  $n$  to 3 in this paper.

With the assumption stated previously, the changing of pixel value and tangential direction along the edges should be minimal. Therefore, we construct a candidate set  $CS_i$  for every extracted verge point  $VP_i(x_i, y_i)$ , by selecting those  $VP_j(x_j, y_j)$  according to the following criterion:

$$\begin{cases} |x_i - x_j| + |y_i - y_j| < T_d \\ |f(x_i, y_i) - f(x_j, y_j)| < T_{int} \\ S(x_i, y_i) \times S(x_j, y_j) > 0 \\ \Delta_{i,j} = |\delta_i| + |\delta_j| < T_\delta \end{cases} \quad (1)$$

where  $\delta_i$  is defined in Fig.2.  $T_d$ ,  $T_{int}$ ,  $T_\delta$  are thresholds to set in implementation. The absolute sum of  $\delta_i$  and  $\delta_j$ , denoted as  $\Delta_{i,j}$  indicates the global change in the tangential direction of  $VP_i$  and  $VP_j$ , which is defined as the cost function in [6] and [9]. In spite of this seemingly strict restraint on pixel value and the consistency of tangential direction, the verge point connection based on minimum  $\Delta_{i,j}$  turns out to be inefficient in practice. In fact, in presence of multiple edges of similar edge direction, the matching factor  $\Delta_{i,j}$  is then less characteristic and results in mismatching of verge points. Therefore, in addition to  $\Delta_{i,j}$ , the matching of neighboring pixel values is taken into consideration.



Fig. 3 Example of edge convergence inside the missing area

We find the best candidate that minimizes the SAD (sum of absolute difference) between the pixels in a small vicinity of  $VP_i$  and those of  $VP_j$ . If its corresponding SAD is smaller than a threshold  $T_{SAD}$ , it is identified as the best match of  $VP_i$  and denoted as  $VP_{i^*}$ . Considering the uniqueness of best match,  $VP_{i^*}$  will be excluded from the succeeding matching process.

$$VP_{i^*} = \arg \min_{VP_j \in CS_i} \sum_{n=0}^N |f(x_{in}, y_{in}) - f(x_{jn}, y_{jn})| \quad (2)$$

where  $f(x_{in}, y_{in})$  and  $f(x_{jn}, y_{jn})$  are pixel values of  $p_{in}$  and  $p_{jn}$  ( $n=1 \dots N$ ) respectively. See Fig. 2 for detailed definition.

The pair connection is performed in a multiple-pixel manner where  $p_{in}$  is linked to  $p_{i^*n}$  ( $n=1 \dots N$ ) accordingly. We linearly link the pair in pixel space as well as in verge point plane. The pixel values of the points between the two end points are reconstructed by linear interpolation between them. Moreover, if they are both verge points and are of the same sign  $S$ , all points between them become verge points and are signed with  $S$ ; the curvature intensity is also interpolated likewise.

### 3.2. Spare verge points

The unmatched verge points of relatively high curvature intensity (over a predefined threshold  $T_{ext}$ ) correspond to edges that end up inside the missing block and thus have no correspondent on borders of the block. As the vicinity of the missing block provide no clue where and how these edges will end within the block, handling these spare verge points prove to be more delicate. Here, we classify the spare verge points into two categories, with respect to whether or not its extension along its tangential angle will join a previously reconstructed verge point in the missing block. For those spare VPs that confront other reconstructed edges, it is extended into the missing block along its tangential angle by simply copying its curvature intensity and its pixel value. Other unmatched VPs exist for several possibilities: 1). Located at the end of an acute object whose edges converge inside the block (see the example in Fig. 3); 2) Changing of curvature direction across the block; 3) Its corresponding verge point on other borders are not extracted due to complicated context. In our algorithm, they are assumed to fade in the block and are thus extended by interpolation. We take the crossing point of its extension along the tangential angle and the block border as the other end point. The pixels between them are obtained by interpolation.

With the reconstructed verge points in corrupted areas, all other missing pixels are recovered by interpolating linearly from the nearest verge points.

#### 4. SIMULATION RESULTS

To compare the performance of the proposed technique with previous algorithms, we applied two error patterns on different pictures (shown in Fig. 4(a) and Fig. 5(a) respectively). All erroneous blocks are sized 16x16, which is the corrupted MB size in video error concealment. TABLE I provides the values of the parameter or threshold adopted in our implementation.

In our simulations, the BI[2] and OASI[7] techniques are selected for performance comparison. The former is the conventional spatial EC method while the latter is known as one of the best techniques in the existing literature especially in terms of PSNR results[7][8]. The comparison results are listed in TABLE II and TABLE III where  $\rho$  is the MB loss ratio. In terms of PSNR, our concealment result is higher or comparable with OASI except for "Lena" in the isolated block loss case. Though its PSNR result is 0.8 dB lower than OASI in this specific case, the subjective perception of "Lena" presented in Fig. 4(e) & (f) prove to be equally satisfactory. In the enlarged area presented in Fig. 6, the edges are reasonably replenished in our concealment, in contrast to the blurring effect caused by BI and OASI. Since our connection of verge points is linear, the reconstructed edges appear to be somehow more abrupt than those of BI. However, the induced picture distortion is hardly perceived and much less than that of OASI. In consecutive block loss case, it is observed in Fig. 5 that our concealment best preserves the contour of the "Lena". Simulations on other images yield similar results.

#### 5. CONCLUSION

We have presented a spatial error concealment technique using the extracted verge points. The verge points surrounding the missing area, though extracted on a pixel basis and from non-immediate neighbors, present faithfully the curvature information in most cases of continuous edges. The proposed method selects the best pairing from a limited number of candidates considering the consistency of both curvature information and neighboring pixel values. Simulations show that in most cases, such pairing criterion recovers edges efficiently.

#### 6. REFERENCES

[1] Y.Wang, S.Wenger, J.Wen, and A.K.Katsaggelos, "Error resilient video coding techniques," *IEEE Signal Processing Mag.*, vol. 17, no. 4, pp. 61-82, July 2000.  
 [2] S.Aign, K.Fazel, "Temporal and spatial error concealment techniques for hierarchical MPEG-2 video codec," in *Proceedings of IEEE International Conference on Communication*, Seattle, 1995, pp. 1778-1783.

[3] W.Kwok, H.Sun, "Multi-directional interpolation for spatial error concealment," *IEEE Trans. on Consumer Electronics*, vol.39, No.3, pp.455-460, Aug.1993.  
 [4] Y. Wang, Q.-F. Zhu, and L. Shaw, "Maximally smooth image recovery in transform coding," *IEEE Trans. Commun.*, vol. 41, No.10, pp. 1544-1551, Oct. 1993  
 [5] J.W.Park and S.U.Lee, "Recovery of corrupted image data based on the NURBS interpolation," *IEEE Trans. on Circuits Syst. Video Tech.*, vol.9 No.7, pp. 1003- 1008, Oct. 1999  
 [6] W.Zeng and B.Liu, "Geometric-structure-based error concealment with novel applications in block-based low-bit-rate coding," *IEEE Trans. on Circuits Syst. Video Tech.*, vol.9 No.4, pp. 648- 665, June 1999  
 [7] X.Li, M.Orchard, "Novel sequential error-concealment techniques using orientation adaptive interpolation," *IEEE Trans. on Circuits Syst. Video Tech.*, vol.12 No.10, pp. 857- 864, Oct.2002  
 [8] M.Chen, M.Wu and Y.F.Zheng, "Classification-based spatial error concealment for images," in *Proceedings of International Conference on Image Processing*, vol.3, pp. 675-678, Sept. 2003  
 [9] L.Atzori, F.G.B De Natale, "Error concealment in video transmission over packet networks by a sketch-based approach," *Signal Process.: Image Commun.*, vol.15, no.1-2, pp.57-76, Sept.1999  
 [10] A.Rareş, M.J.T.Reinders and J.Biemon, "Edge-based image restoration," *IEEE Trans. on Image Processing*, vol.14 No.10, pp.1454-1468, Oct.2005  
 [11] S.J.Wang, L.C.Kuo, H.H.Jong et al., "Representing images using points on image surfaces," *IEEE Trans. on Image Processing*, vol.14 No.8, pp.1043-1056, Aug.2005  
 [12] G.Sapiro and D.L. Ringach, "Anisotropic diffusion of multi-valued images with applications to color filtering," *IEEE Trans. on Image Processing*, vol.5, No.11, pp.1582-1586, Nov.1996

**TABLE I**  
ADOPTED VALUE FOR PARAMETERS IN IMPLEMENTATION

Parameter	$T_d$	$T_{int}$	$T_\delta$	$N$	$T_{SAD}$	$T_{ext}$
Value	50	30	0.6	5	100	15

**TABLE II**  
PERFORMANCE COMPARISON IN PSNR FOR THE ISOLATED BLOCK LOSS CASE ( $\rho=7.9\%$ )

PSNR(dB)	Lena	Pepper	House	Foreman
BI	24.32	24.07	23.01	25.53
OASI	25.81	26.45	24.43	27.71
Ours	24.97	26.60	25.46	27.90

**TABLE III**  
PERFORMANCE COMPARISON IN PSNR FOR THE CONSECUTIVE BLOCK LOSS CASE ( $\rho=23.7\%$ )

PSNR(dB)	Lena	Pepper	House	Foreman
BI	22.12	23.66	21.16	22.24
OASI	22.70	23.35	21.82	24.13
Ours	22.81	23.37	21.94	24.17



Fig. 4 Recovery of isolated block loss ( $\rho=7.9\%$ ): (a) Corrupted image; (b) Concealed with BI[2], 24.32dB; (c) Extracted verge points from (a); (d) Reconstructed verge points; (e) Concealed with OASI[7], 25.81dB; (f) Concealed with the proposed method, 24.97dB

Fig. 5 Recovery of consecutive block loss ( $\rho=23.7\%$ ): (a) Corrupted image; (b) Concealed with BI[2], 22.12dB; (c) Extracted verge points; (d) Reconstructed verge points; (e) Concealed with OASI[7], 22.70dB; (f) Concealed with the proposed method, 22.81dB

\* In implementation, only relevant verge points are extracted. The picture-wise verge points in (c)&(d) are presented to illustrate the result of verge point reconstruction. VPs of positive signs are presented in black and those of negative sign in gray.

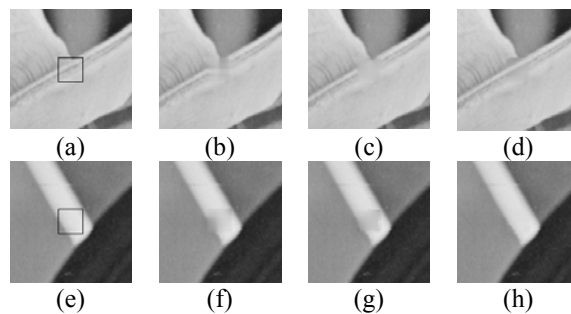


Fig. 6 Zoomed view of Fig. 4: (a)&(e) Original picture; (b)&(f) Concealed with BI[2]; (c)&(g) Concealed with OASI[7]; (d)&(h) Concealed with the proposed method